Supplementary Material - Nitrogen Availability and Summer Drought, but not N:P Imbalance Drive Carbon Use Efficiency of a Mediterranean Tree-Grass Ecosystem

S1: Effect of variable u* threshold

We used data as processed in (El-Madany et al., 2018; El-Madany et al., 2021). This included a variable u* threshold per site per year following (Papale et al., 2006). In short, a variable u* was calculated independently for three four monthly periods within the year. Conservatively, the highest value from any period in each year was used for the entire calendar year. In Figures S1.1 and S1.2 we show the equivalent of Figure 2c and 4c with both the 'standard' u* partitioning used in the main manuscript and two alternate static thresholds, a 'low' threshold (0.12 ms-1) and a 'high' threshold (0.2 ms-1) which were derived from the distribution of the periodic calculated thresholds. In all cases the difference between this choice of u* threshold in the processing step was smaller than the nutrient treatment effect, and also smaller than seasonal variation.

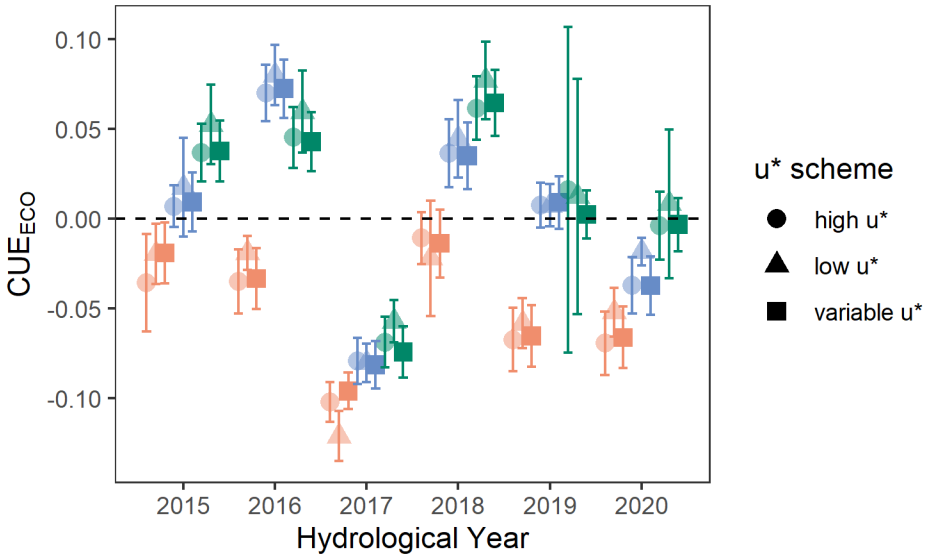

Figure S1.1: Effect of alternate u* schemes on annual CUE. Both high and low u* threshold effects were smaller than the difference between treatments. Colours are nutrient treatments as in Fig. 2c.

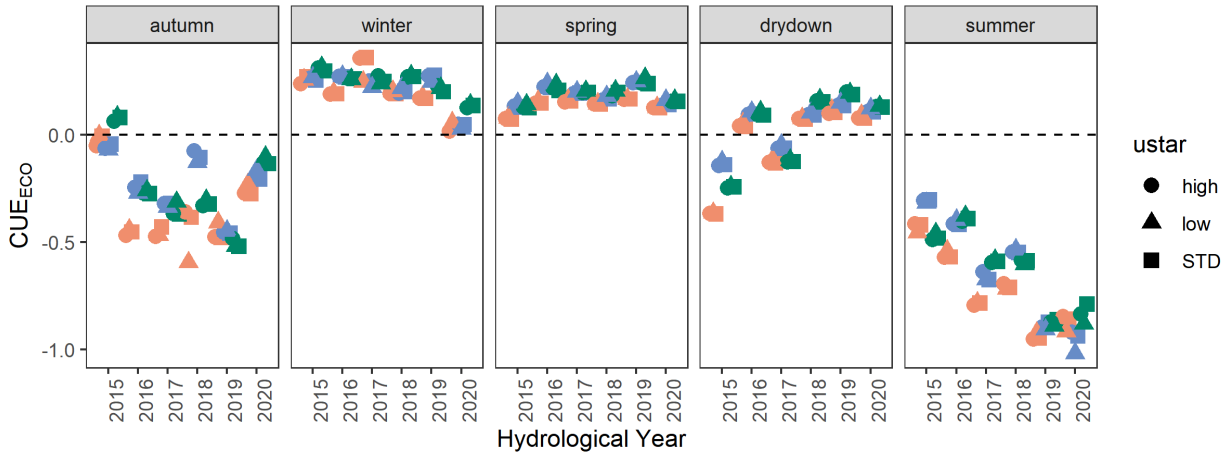

Figure S1.2: Effect of alternate u* schemes on seasonal CUE. Both high and low u* threshold effects were smaller than the difference between treatments and seasons. Colours are nutrient treatments as in Fig. 4c.

S2. Season Assignment

We assigned seasons based on PTDs: Phenological transition dates from phenocam timeseries. PTDs and seasons are difficult to estimate from more continental Mediterranean locations because of the presence of an interruption in the growing season which can result in two, or one conjoined greenness peak. Summer is also not well defined by a particular peak.

We assigned seasons by extracting PTDs separately for each treatment following (Luo et al., 2018) and assigning each date to the nearest PTD of interest. PTDs were based on the green chromatic coordinate (GCC) from phenocam image.s These were as follows: Autumn: SOS50 (the midpoint of the rising curve at the start of the hydrological year), Winter: InterminD (the lowest point between two peaks), Spring: POS2 (the second peak), Drydown: EOS50 (the midpoint of the falling curve at the end of the hydrological year). We assigned summer based on the date midway between the start of drydown (EOS25) and the PTD at the start of autumn in the next year (EOS25). An example of these assignments is given in Fig. S2.

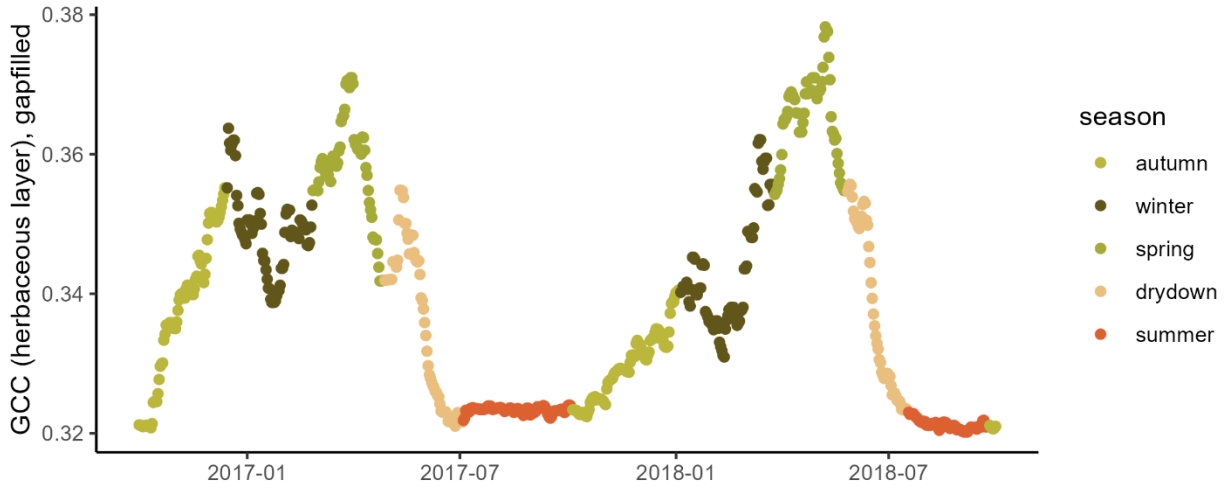

Figure S2 – Demonstration of seasonal assignment using our GCC (green chromatic coordinate)-based scheme across two calendar years in the control treatment; a dry autumn and winter in 2017 meant the GCC phenological curve had a different shape.

S3: PCA on instantaneous meteorology

We conducted a PCA on the instantaneous meteorological variables (VPD, Tair, RH, PAR, and Daytime VPD and RH) to construct our 'Dim1' meta-variable for the GAM analysis. This was because there was a high expectation of autocorrelation between these variables at the daily scale. Indeed, the contribution of these variables to PC1 was 92 % and the loadings of the variables were all close to 1 in either the positive (VPD, Tair, PAR) or negative (RH) direction (Fig. S2.1).

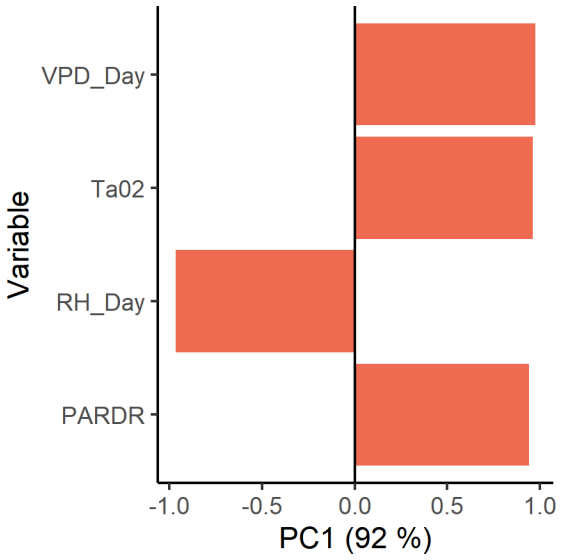

Figure S3. Loadings of the main principle component of the instantaneous meteorology PCA.

S4: Hydrological year variation, meteorology and calendar controls

As well as the controls on CUE_{ECO} which we show in the main manuscript depending on year length, the length of the hydrological year was primarily controlled by the summer drought period (Spearman's rank, coef. = 0.80, Fig. S3).

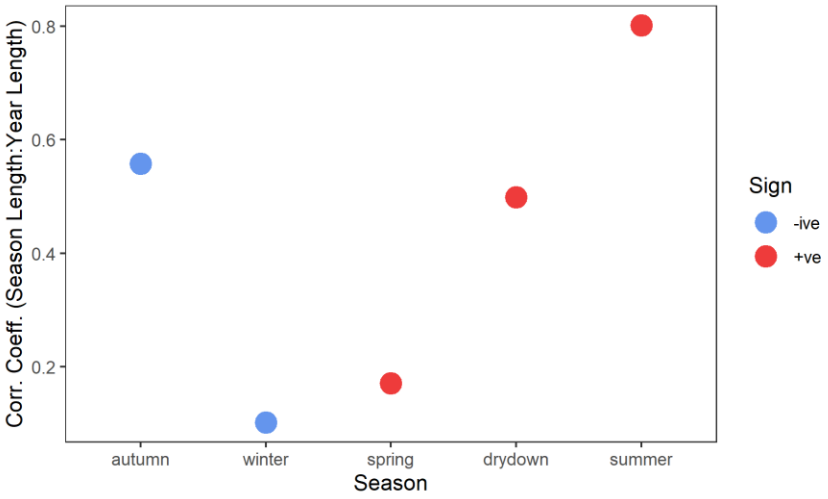

Figure S3: Spearman's rank correlation coefficients between the length of season and the length of year. The length of the year was primarily controlled by how long the summer drought lasted; the most highly correlated were a positive effect of summer length and a negative effect of autumn length.

S5: Trends in Environmental Variables

Because phenology dominates functioning of all ecosystems, there was a strong seasonal cycle of all environmental variables. 'Meteorology' (Fig. S2a) was higher (e.g. hotter, dryer) in summer than winter. Correspondingly, SWCn (Fig. S2b) and CSWI (Fig. S2c) followed similar patterns, SWC changing more on short timescales due to rain. NDVI also followed phenology Fig. S2d). Importantly, because NDVI, soil moisture content and footprint meteorological variables were measured on a per-treatment basis, these could differ between treatments at the same time. There were visible treatment effects on NDVI and SWC; the control treatment tended to have a lower NDVI in summer and winter and water availability differed between the treatments.

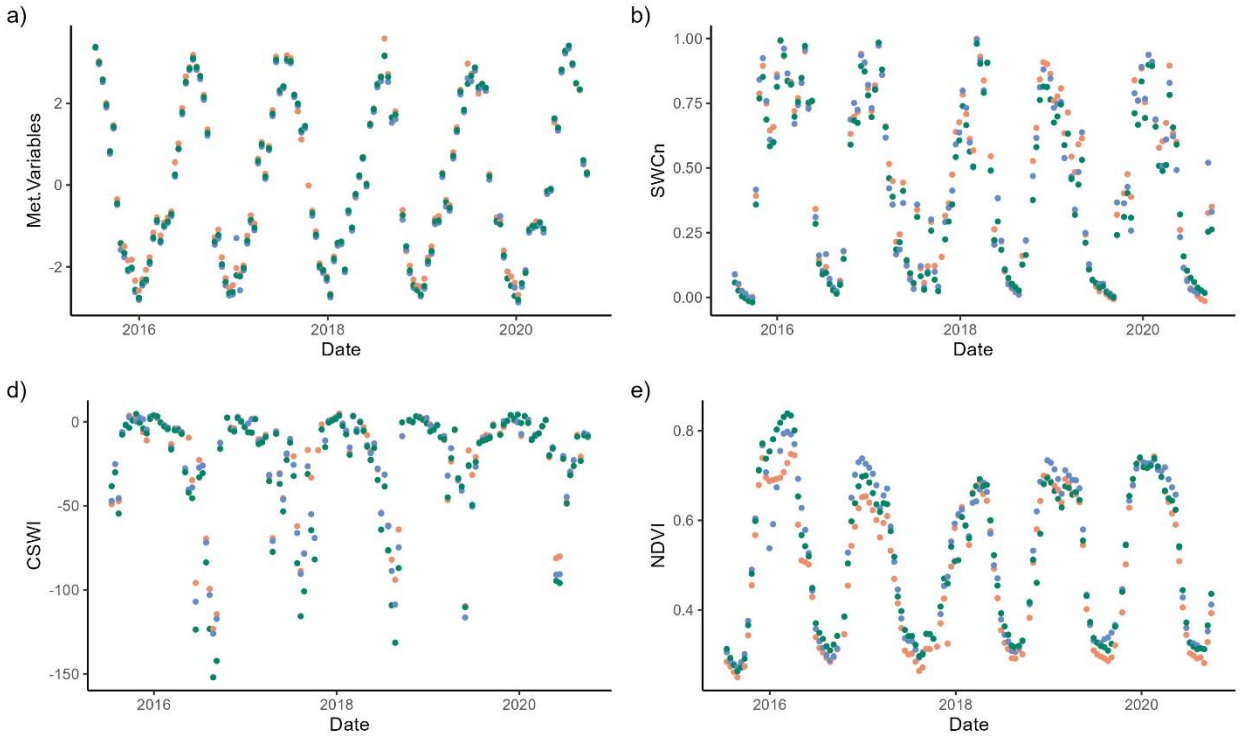

Figure S5 – Overall trends in the variables used in the best fitting GAM., Met Variables, the combind variable from the principle component analysis (a) had some minor variations due to micrometeorology i.e. VPD and RH) measured between sites. SWC (b) had treatment differences even when normalized; notably, the NT treatment was a little drier,

especially in late spring and drydown. This was also reflected in CSWI (c). NDVI (d) was also higher in the nutrient fertilized treatments, including in summer.

S6: Seasonal Transition Capture

Our assignment of phenological seasons from transition date meant to some extent we avoided problems with lagged responses in biological responses to meteorological change. In particular these lags affect autumn because microbial activity is limited by water and can only occur in summer following rain pulses. A key weakness of a model which does not include a time series legacy representation is incorrect attribution of the lagged link between productivity and respiration. However, the PTD-season assignment meant we only started 'autumn' once vegetation had begun to green up. Hence to some extent, we were able to attribute some of the end of summer respiration peaks to the correct vegetation-season. (Fig. S5).

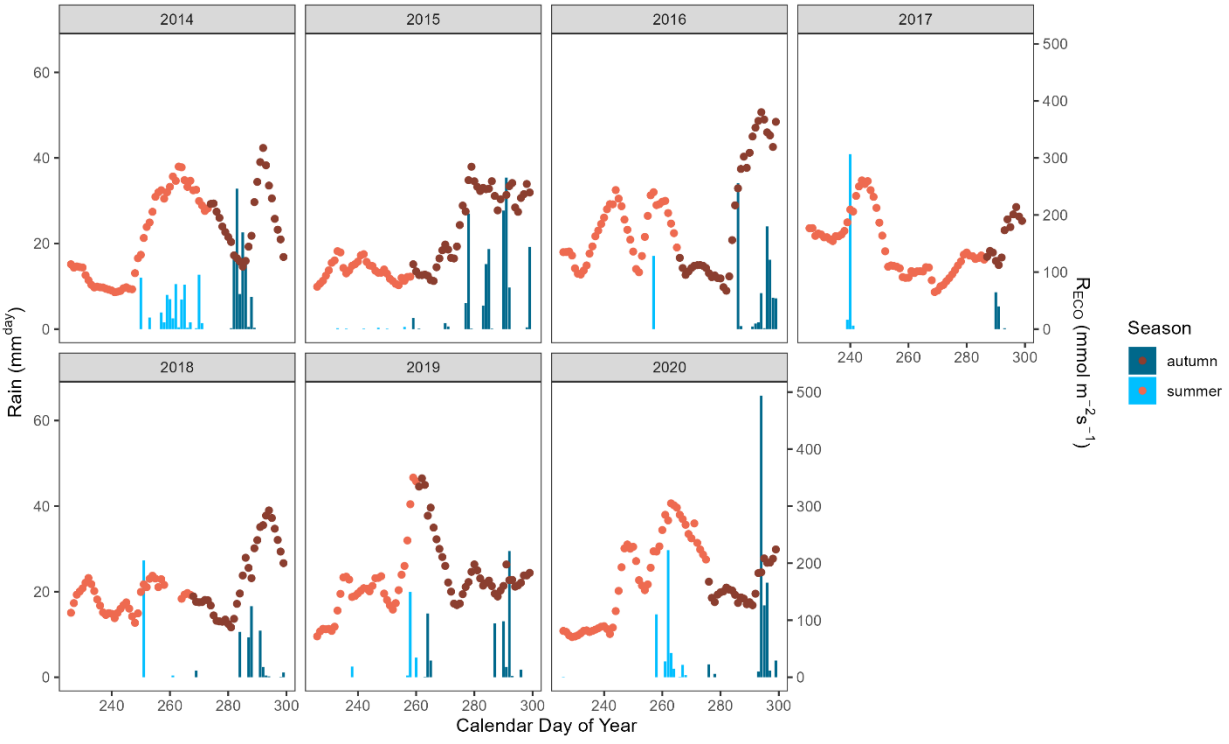

Figure S5: Daily rainfall and R_{ECO} for end of year (calendar DOY 225-300) for seven hydrological years in the NT treatment. Using our vegetation phenology-based scheme we usually captured a rain pulse and a corresponding CO_2 efflux at the end of summer which allowed vegetation to green up and begin signalled our autumn transition. Notably

this was not the case in 2015 - where the autumn was very wet and 2018 -where the end of the previous year was very dry.

El-Madany, T. S., Reichstein, M., Carrara, A., Martín, M. P., Moreno, G., Gonzalez-Cascon, R., Peñuelas, J., Ellsworth, D. S., Burchard-Levine, V., Hammer, T. W., Knauer, J., Kolle, O., Luo, Y., Pacheco-Labrador, J., Nelson, J. A., Perez-Priego, O., Rolo, V., Wutzler, T., & Migliavacca, M. (2021). How Nitrogen and Phosphorus Availability Change Water Use Efficiency in a Mediterranean Savanna Ecosystem. *Journal of Geophysical Research: Biogeosciences*, *126*(5), e2020JG006005. https://doi.org/10.1029/2020JG006005

El-Madany, T. S., Reichstein, M., Perez-Priego, O., Carrara, A., Moreno, G., Pilar Martín, M., Pacheco-Labrador, J., Wohlfahrt, G., Nieto, H., Weber, U., Kolle, O., Luo, Y. P., Carvalhais, N., & Migliavacca, M. (2018). Drivers of Spatio-Temporal Variability of Carbon Dioxide and Energy Fluxes in a Mediterranean Savanna Ecosystem. *Agricultural and Forest Meteorology*, *262*(July 2017), 258–278. https://doi.org/10.1016/j.agrformet.2018.07.010

Luo, Y., El-Madany, T. S., Filippa, G., Ma, X., Ahrens, B., Carrara, A., Gonzalez-cascon, R., Cremonese, E., Galvagno, M., & Tiana, W. (2018). Using Near-Infrared-Enabled Digital Repeat Photography to Track Structural and Physiological Phenology in Mediterranean Tree – Grass Ecosystems. *Remote Sensing*, *10*, 1293. https://doi.org/10.3390/rs10081293

Papale, D., Reichstein, M., Aubinet, M., Canfora, E., Bernhofer, C., Kutsch, W., Longdoz, B., Rambal, S., Valentini, R., Vesala, T., & Yakir, D. (2006). Towards a standardized processing of Net Ecosystem Exchange measured with eddy covariance technique: Algorithms and uncertainty estimation. *Biogeosciences*, *3*(4), 571–583. https://doi.org/10.5194/bg-3-571-2006